arXiv:1611.01851v1 [cs.RO] 6 Nov 2016

Optimal Spline Trajectories by Modelling Kinematic Constraints in Robot Soccer

Abhinav Agarwalla[1], Arnav Kumar Jain[1], Arpit Saxena[2], Jayanta Mukhopadhyay[2]

***Abstract*— We explore optimal motion planning and control for a soccer playing differential drive robot. Trajectories generated using end-slope cubic Bézier splines are optimised globally through Bayesian optimisation and locally through Nelder-Mead downhill simplex method. A velocity profile for the trajectory is generated incorporating kinodynamic constraints of the robots. Control point optimisation resulted in minimum time trajectories while respecting robot constraints. A novel trajectory tracking algorithm for differential drive robots is also developed which accounts for transmission delay. Gauss-Kronrod numerical integration, Newton Rhapson and other numerical methods have been employed for computational efficiency, keeping in mind the highly dynamic robot soccer environment. Extensive testing on developed simulator, as well as on our robot soccer team, has shown marked improvements in stability and speed over other techniques.**

I. INTRODUCTION

One of the prime tasks in motion planning is determination of optimal trajectory between source and destination in the traversable region. It is very crucial in robot soccer, where high level complex maneuvers like attacking and passing are performed through coordination of multiple robots. A highly dynamic environment with an opponent team trying to beat one team on the same task makes this even more challenging. We define optimal trajectory as one which enables fastest traversal while obeying kinematic constraints of the robot. High deviations from the generated trajectory i.e. high tracking errors of mobile robots cause slipping and collisions with opponents which is highly undesirable. It also increases travelling time and distance, resulting in sub-optimal traversal. Trajectories that take into account limits on velocity and acceleration result in very small deviations from the path.

Traditional approaches such as PolarBased[1], MergeSCurve[2], Proportional Controller[3], CMUnited controller[4] and Dynamic Window[5][6] have several pitfalls, most important to us being: (1) sub-optimal traversal due to being reactive in nature, (2) no guarantees and estimates of travel time and distance leading to inefficient high level behaviours, (3) no incorporation of kinodynamic constraints of the bot (except Dynamic Window) and (4) frequent slipping of wheels at high speed. Trajectory based methods generally use Bézier curves [7],[8], B-splines[9] or Quintic Bézier Splines[10] for trajectory generation along with building velocity profiles that incorporate kinodynamic constraints. Our work[1] builds on work by Shiller and Gwo[9], and Lau et al. [10]. We use cubic Bézier splines for trajectory generation and optimise it globally using Bayesian Optimisation[11] and locally by Nelder-Mead simplex[12] method. A linear tracker uses vision data, and optimised trajectory for sending robot velocity as depicted in Fig. 1.

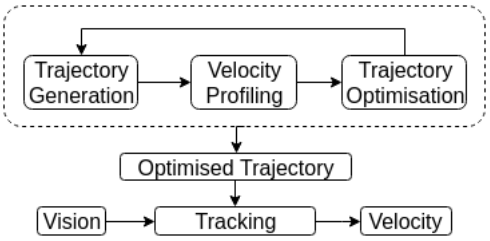

Fig. 1. Planning Overview: Initial trajectory generated is optimised using trajectory optimisation, after velocity profiling. Using the optimised trajectory and vision input, tracker calculates and sends robot velocities.

This paper is organised as follows: Section II describes the overall system and kinodynamic constraints on the robot while Section III introduces spline trajectory generation. Section IV discusses incorporation of velocity and acceleration constraints through velocity profiling. Section V and Section VI describe trajectory optimisation and tracking module, respectively. Section VII discusses and compares results of various motion planning algorithms followed by conclusion in Section VIII.

II. ROBOT DYNAMICS

Federation of International Robot-Soccer Association (FIRA)[2] organises Mirosot league every year, in which a team of five mobile robots compete against an opponent team to win a soccer match. The playing field is a rectangle with 2.2m width and 1.8m height. A Mirosot robot is a differential drive robot with two wheels on the sides and supportive caster wheels on the front and back. The robot has zero turn radius, and can rotate only about its geometric center. The robot is fitted inside a cube with sides of length 7.5cm. Due to this physical constraint, there is no possibility of inclusion of a kicker or dribbler mechanism in the robot, implying that the only way to score a goal is to intercept the ball from behind and drag the ball into the goal.

This work was supported by Sponsored Research and Industrial Consultancy, Indian Institute of Technology, Kharagpur

[1]Department of Mathematics,Indian Institute of Technology, Kharagpur, India {abhinavagarwalla,arnavkj95}@iitkgp.ac.in

[2]Department of Computer Science and Engineering,Indian Institute of Technology, Kharagpur, India {arpitt.saxena,jay}@cse.iitkgp.ac.in

[1]https://github.com/abhinavagarwalla/motion-simulation

[2]https://www.fira.net/

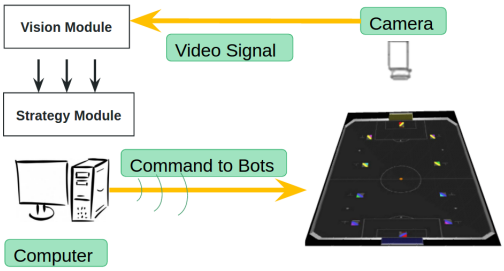

Fig. 2. System Setup and Overview

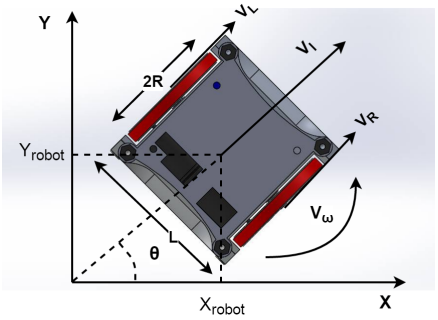

Fig. 3. Robot Kinematic Model. (x, y, θ, v_l, v_w) constitute robot state

The system setup is described in Fig. 2. A central server takes in feed from the overhead camera, and extracts the position, orientation and velocity of our robots as well as opponent robots using SSL-Vision[13]. Raw values are passed through either Kalman[14] filter or Savitzky Golay[15] filter to eliminate the acquired noise. The server calculates the velocities to be sent to the robot according to the game play and tracker. The camera captures an image every 16ms, thereby updating ball and robot state. A XBee-PRO module then transmits the velocities to the micro-controller fitted on each robot. There is an internal Fuzzy-PID[16] loop running on the motors, which decides the velocity of motors.

A. Kinematics

A differential drive robot has two wheels on each side, each of which can rotate independently. The motion behaviour of the robot is determined by velocity of the wheels, which is controlled by a motor attached to each wheel. A kinetic model of the robot is described in Fig. 3. The linear velocity v_l and angular velocity v_ω of robot is expressed in (1), where v_L, v_R, and l are the left wheel velocity, right wheel velocity and the distance between wheels, respectively.

$$v_l = \frac{v_L + v_R}{2}, v_\omega = \frac{2(v_R - v_L)}{l} \tag{1}$$

Equation (2) describes the relation of linear and angular velocities with position coordinate (x, y) and orientation θ of the robot.

$$x' = v_l cos(\theta), y' = v_l sin(\theta), \theta' = v_\omega \tag{2}$$

Robots have a high tendency to slide in a robot soccer game due to sharp turns at high velocities and reduced ground friction. In case of slipping, (2) can no longer describe its motion. Though physical solutions like using rubber bands on wheels and keeping low centre of gravity are employed, velocity and acceleration constraints must be addressed in the planning algorithm to avoid slipping of the robot.

B. Physical Constraints

1) Velocity Constrains: The wheels have a diameter of 5.2 cm and they are 7 cm apart. High torque and high RPM Faulhaber motors are used. Taking account of the robot dimensions, Fuzzy-PID control loop, circuit design and motors specifications, the maximum loaded velocity attainable by the robot is 200 cm/s.

2) Acceleration Constraints: The maximum acceleration a_{max} of the robot is limited by the friction coefficient $c_{friction}$ as follows:

$$a_{max} = \frac{F_{friction}}{m} = g c_{friction} \tag{3}$$

where m and g are mass of the robot and gravitational acceleration, respectively. The acceleration of the robot is composed of tangential component a_{tang} and radial component a_{rad} as given by (4).

$$a_{tang} = \frac{dv_l}{dt}, a_{rad} = v_l v_\omega \tag{4}$$

Since the tangential and radial accelerations are orthogonal, the total acceleration is given by:

$$a = \sqrt{a_{tang}^2 + a_{rad}^2} \tag{5}$$

For calculating the radial acceleration, the robot is run on a circular path with a fixed radius as in [17]. The value of a_{rad} is increased in steps till the slipping point. The maximum a_{rad} is logged for different radius values of the circular path. Using linear regression, radial acceleration is obtained as a function of radius of curvature r, given by (6).

$$a_{rad} = -5.92r + 700 \tag{6}$$

III. TRAJECTORY GENERATION

Cubic Bézier Splines[18] are chosen to represent trajectories because of their desirable smoothness properties. Two dimensional paths are obtained by parametrization of path along x and y directions through the parameter u along the curve using ALGLIB[19]. Initial trajectory is generated by stitching together n segments of Cubic Bézier Splines along the $n-1$ control points. The coordinates of these control points are heavily optimised as described in the next section. The equation for the Cubic Bézier Splines is given by (7), which follows the continuity and differentiability constraints at the knots in (8), (9) and the boundary conditions in (10). Initial robot velocity, as captured from the overhead camera, after accounting for packet delay is incorporated in (11) resulting in formation of end slope cubic splines. B_i denotes i^{th} segment of the spline, whereas P_{i0}, P_{i1}, P_{i2}, and P_{i3} are coefficients.

$$B_i(u) = \begin{bmatrix} (1-u)^3 \\ 3(1-u)^2u \\ 3(1-u)u^2 \\ u^3 \end{bmatrix}^T \begin{bmatrix} P_{i0} \\ P_{i1} \\ P_{i2} \\ P_{i3} \end{bmatrix} \tag{7}$$

$$B_i(1) = B_{i+1}(0) \tag{8}$$

$$B_i^{'}(1) = B_{i+1}^{'}(0), B_i^{''}(1) = B_{i+1}^{''}(0) \tag{9}$$

$$B_i(0) = P_{i0}, B_i(1) = P_{i3} \tag{10}$$

$$B_i^{'}(0) = v_l(0), B_i^{'}(1) = v_l(1) \tag{11}$$

Quintic Bézier Splines[10] are also explored which have the additional property of curvature continuity at end points. They are compared with their cubic counterparts in terms of trajectory traversal time, tracking error and average velocity of the robot. The method is inherently bidirectional by taking account of the direction of velocity at the time of trajectory generation.

A. Arc Length

Since we have two Cubic splines, parametrised by parameter u, numerical integration is the preferred way to calculate arc-length. Arc-length is given by (12), where B_x, B_y denote splines along x and y direction.

$$S = \int_{u_1}^{u_2} \sqrt{B_x'(u)^2 + B_y'(u)^2} du \tag{12}$$

Arc length is computed using Gauss-Kronrod 21-point integration rule using Quadrature Adaptive General Singularity (QAGS)[20] routine implemented in GNU Scientific Library[21], which speeds up integration of integrable singularities.

B. Arc Length Re-parametrisation

Arc length re-parametrisation is required to compute the parameter u from the arc length S, which is achieved through approximating the function $u(S)$. Re-parametrisation is implemented through Bézier splines[22] and inverting Bézier curves[23], of which former is finally chosen due to better performance. Equidistant points are sampled from $u \in [0, 1]$, and arc length on each of these points is computed using (11). Then, a 1D Cubic Bézier Spline is fitted on these points, approximating u as a function of S. Now, getting the corresponding u for a given arc length, is a simple evaluation of the cubic spline at u.

IV. VELOCITY PROFILING

To completely describe its motion, we also need to set the velocity to be achieved at each point on the generated trajectory. Velocity profile must be generated incorporating robot dynamics to minimise the error between observed and expected position at any moment of time. While keeping the errors to minimum, we also need to find the fastest way to complete the trajectory. This translates to maximising velocity at each point while respecting the kinodynamic constraints.

On the trajectory $B(u)$, we fix a set of N_c equidistant planning points p_i along the arc length. Planning points are just sampled from the generated trajectory. We have assumed that the acceleration between two planning points p_i and p_{i+1} is constant, which holds true for most trajectories in practice due to selection of sufficiently many points. Each translational velocity v_i corresponds to a planning point p_i.

A. Constraints

The kinodynamics constraints limits the maximum velocity v_i that can be set at each planning point p_i.The maximum translational velocity $v_{max|\omega}$ at a point p_i is given by (13), where ω_{max} and κ_i denote maximum rotational velocity and curvature at that point, respectively.

$$v_i \in [0, v_{max|\omega}], v_{max|\omega} = \frac{\omega_{max}}{|\kappa_i|} \tag{13}$$

The acceleration constraints at any planning point p_i depends on the velocities of the adjacent points p_{i-1} and p_{i+1}. The acceleration constraints are symmetric for the motion planning to be smooth and to avoid slipping of the robot. At any planning point p_i, $v_i \in [v_{min|a_t}, v_{max|a_t}]$ can be attained using:

$$v_{min|a_t} = v_{i-1} - a_{t_{max}}\Delta_t \tag{14}$$

$$v_{max|a_t} = v_{i-1} + a_{t_{max}}\Delta_t \tag{15}$$

The boundary conditions can now be obtained for translational velocities obeying $a_{t_{max}}$, where distance between any two planning points p_i, p_{i+1} is Δ_s. The reader can refer to [24] for complete details.

$$v_{min|a_t} = \begin{cases} \sqrt{v_{i-1}^2 - 2a_{t_{max}}\Delta_s} & v_{i-1}^2 \geq 2a_{t_{max}}\Delta_s \\ 0 & else \end{cases} \tag{16}$$

$$v_{max|a_t} = \sqrt{v_{i-1}^2 + 2a_{t_{max}}\Delta_s} \tag{17}$$

B. Profile Generation

Initial velocity v_0 is set to initial velocity of robot. Final velocity v_{N_c} is set according to the individual robot behaviour, whether the role assigned to the robot is an attacker, defender or goalkeeper. Forward consistency is established by accelerating with the maximum constrained acceleration from point p_i to reach p_{i+1} with maximum velocity. The process is repeated in the reverse direction. This ensures that the robot traverses between any two points obeying the constraints. The total time needed to complete the trajectory can be easily calculated, once the velocity v_i at each planning point p_i is determined.

V. TRAJECTORY OPTIMISATION

We reduce the problem of finding optimal path to the problem of optimising over curvature and time of the trajectories. It is important to reduce the curvature of the generated trajectory, since high curvature paths result in either reduced robot speeds or high chances of wheel slipping. Wheel slipping also results in inability to track the generated trajectory. In a robot soccer match, there is always a race between the teams to be the first to reach the ball, thus motivating the need for optimisation with respect to time.

A. Maximum Curvature Calculation

The curvature for the parametrized splines is given by (18), where the values of $x'(u)$, $x''(u)$, $y'(u)$ and $y''(u)$ can be easily calculated by differentiating spline equation (7).

$$\kappa(u) = \frac{x'(u)y''(u) - y'(u)x''(u)}{(x'(u)^2 + y'(u)^2)^{\frac{3}{2}}} \tag{18}$$

One way to calculate the maximum curvature is to evaluate the curvature at points obtained after uniform sampling of the spline parameter u along the curve arc length. Though this method is simple, but it is very computationally expensive. Since the curvature is differentiable, Newton-Raphson[25] technique is used for finding the maximum curvature. Since Newton-Raphson technique is a root finding technique, we look for roots of $\kappa'(u)$ given by (29) in Appendix A. The iteration is continued until the difference in curvature values is less than a threshold or the computation time is exceeded.

$$u_2 = u_1 - \frac{\kappa'(u_1)}{\kappa''(u_2)} \tag{19}$$

B. Computation of Traversal Time

Assuming that the acceleration is constant between the two planning points p_i and p_{i+1}, we compute the time taken to reach any of the equidistant planning points using (20), where v_i and v_{i+1} are determined from velocity profile. The time at the end point gives the total time for the trajectory, given by (21).

$$t_{i+1} = t_i + \frac{2\Delta_s}{v_i + v_{i+1}} \tag{20}$$

$$totalTime = t_{N_c} \tag{21}$$

C. Obstacle Avoidance

Since robots move at high velocity in a soccer game, not incorporating obstacle avoidance sometimes leads to permanent damage of the robots. In our case, obstacle avoidance is simply achieved through adding a large negative value in case the current trajectory intersects an opponent robot. This results in the optimisation step rejecting the trajectory itself. The field boundaries are also taken as line obstacles, resulting in rejection of any trajectory outside the soccer field.

Velocity profiles restrict the maximum velocity on curved paths, thus ensuring that trajectories with high curvature are penalised through increased traversal time. In this way, optimisation over curvature is implicitly handled by optimising over time. The objective F is set to minimise total time (21) depending on the position of 2 control points denoted using four variables: $CP_{1,x}$, $CP_{1,y}$, $CP_{2,x}$ and $CP_{2,y}$. For $CP_{i,j}$, i denotes i^{th} control point and j denotes coordinate axis, as given by (22).

$$F(x = \{CP_{1,x}, CP_{1,y}, CP_{2,x}, CP_{2,y}\}) = totalTime(getTrajectory(x)) \tag{22}$$

Since F is a computationally expensive nonlinear function for which closed form computation or gradient calculation are not possible, Bayesian optimisation[11] is employed. Bayesian optimisation as discussed in Algorithm 1, is a very sample efficient as it decides the next point to evaluate the objective F on a criterion C based on the distribution of function space using a prior. For our case, total traversal time is taken as objective function F, Expected Improvement[26] as criterion C, and Gaussian Process[27] as the surrogate model for prior with Automatic Relevance Determination(ARD) Matérn 5/2 kernel[26]. An initial set X of points are sampled using Latin hypercube sampling[28] which generates random numbers from a stratified input distribution. The surrogate model is incrementally updated to encode the observation history, from which the point maximising criterion is selected as next evaluation point.

For finding the optimal placement of the control points, we first optimise it globally through Bayesian optimisation for various combinations of starting and ending point. A database is formed, which stores the optimal placement of control points for a given starting and ending point. For trajectory planning during a match, Nelder-Mead simplex[12] method is initialised using optimum control point positions from the database. It then optimises trajectory locally till either convergence is achieved or computation time runs out.

Data: startPos, endPos, startVel, endVel
Result: B^* is the optimal trajectory
$X = \{x_1, x_2, x_3...\}$ using Latin Hypercube Sampling;
n = number of dimensions = 4;
maxRange = 1000;
$x_i \in (\mathbb{R} \cap [-maxRange, maxRange])^n$;
Objective $f(x) = totalTime(getTrajectory(x))$;
$y = \{f(x_1), f(x_2), f(x_3), \dots\}$;
$D = \{X, y\}$;
Best $x^* = \underset{x}{\operatorname{argmax}}\ y$;
Criterion $C(x) = \mathbb{E}[\max(0, f(x) - f(x^*))]$;
$d = |x_1 - x_2|$;
Kernel $K(x_1, x_2) =$
$\sigma^2(1 + \sqrt{5\sum_1^n \frac{d^2}{l_i^2}} + \frac{5}{3}\sum_1^n \frac{d^2}{l_i^2}) \exp(-\sqrt{5\sum_1^n \frac{d^2}{l_i^2}})$;
Prior $P(f) \sim \mathcal{GP}(0, K(\theta = \{l_i \dots, l_n, \sigma\}) + \sigma_n^2 I)$;
while $iter < n_{iter}$ **do**
  Update $P(f|D) \propto \int P(D|f,\theta)P(f)P(\theta)d\theta$;
  Select $x_i = \underset{x}{\operatorname{argmax}}\ C(x|P(f|D))$;
  $\{X, y\} = \{X, y\} \cup \{x_i, f(x_i)\}$;
end
B^* = getTrajectory(x^*);

Algorithm 1: Trajectory optimisation using Bayesian optimisation

VI. Tracking

The tracking module ensures that the robot follows the trajectory by minimising the error between the current robot state and the expected state at that moment of time. The current tracker is very similar to [29] with incorporation of packet delay. Characteristic frequency $\omega_n(t)$ of the system is given by (23) where v_r, ω_r are tangential and angular velocity, respectively. Controller gains k_1, k_2, k_3 are given by (24) where ζ represents damping coefficient, and g is

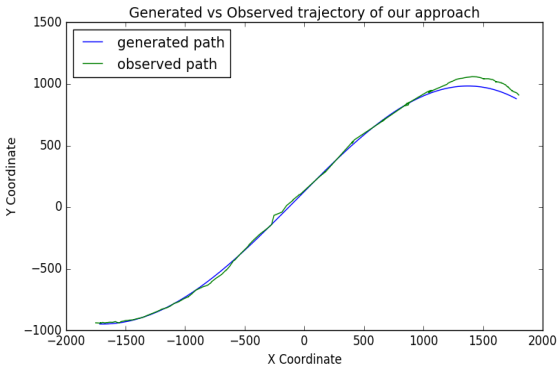

Fig. 4. Blue line represents the generated spline trajectory, while green line represents the trajectory followed by the robot

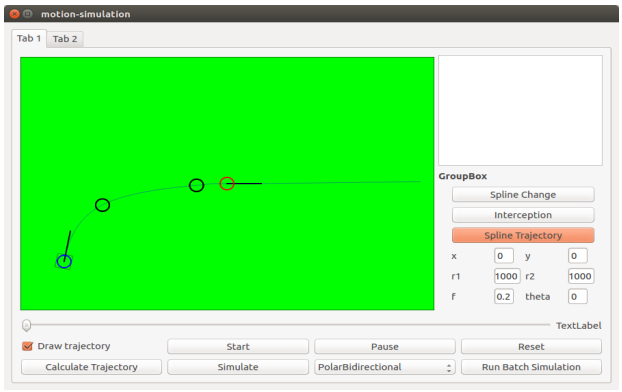

Fig. 5. Simulator developed for testing and debugging

simply a parameter. Errors in position (x, y), orientation θ, and feedforward tangential and angular velocity are denoted by e_1, e_2, e_3, u_{r1} and u_{r2} respectively. The final tangential velocity v and angular velocity w sent to the bot are given by (25) and (26) respectively. Fig. 4 visualises its performance for a cubic Bézier spline trajectory.

$$\omega_n(t) = \sqrt{\omega_r(t)^2 + g v_r(t)^2} \tag{23}$$

$$k_1 = k_3 = 2\zeta\omega_n(t), k_2 = g|v_r(t)| \tag{24}$$

$$v = u_{r1} cos(e_3) + k_1 e_1 \tag{25}$$

$$w = u_{r2} + sgn(u_{r1}) k_2 e_2 + k_3 e_3 \tag{26}$$

A. Trajectory Update

The tracking error might become very large due to either large deviation from the generated path because of slipping of wheels, or collision with another robot. In addition, the destination point changes frequently because of highly dynamic environment. An updated trajectory is generated in response to such situations. Also, the mobile robot does not receive the sent velocities instantaneously. There is a time lag between transmitting and receiving of packets which we define as packet delay, and was calculated to be 4 packets i.e. 64ms. We generate new trajectories while compensating for this delay. The current robot position is chosen as the starting point of the new trajectory and the trajectory is made to pass through the predicted position of the robot 4 packets later. Using the velocity profile of the current trajectory, we can determine the robot velocity after 4 packets which is set as initial velocity for updated trajectory for satisfying (11). This ensures continuity and smooth transitions from current to updated trajectory.

VII. Results and Discussion

A simulator is developed for the purpose of testing the locomotion algorithms as shown in Fig. 5. It is specially designed to enable simulation with kinematic and physical model of Kharagpur RoboSoccer Students' Group (KRSSG) Mirosot robots. The dimensions of the simulated robots, and actuator limits are set as the same as that of actual robots. It

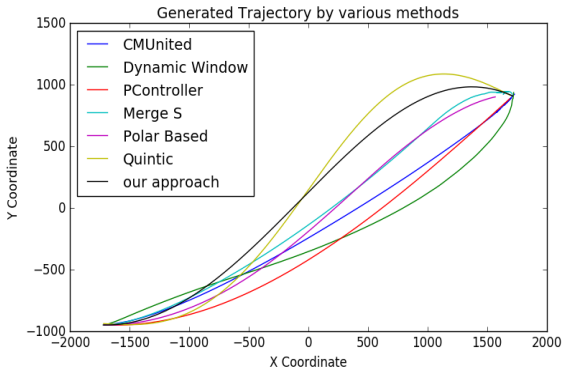

Fig. 6. Comparison of generated trajectories of various controllers

discretises the transmission into steps of 16ms, accounts for packet delay and adds noise as encountered while working on real robots. Different algorithms are first designed and tested on the simulator, and then on actual robots. Due to the special care taken in designing the simulator, only minimal retuning of parameters is required and the same code works on both the simulator and the real robots. This has also proved useful in fine-tuning of parameters in the simulation itself.

We plan a fixed maneuver for the robot comprising of a set of 10 starting and ending positions. The task of the robot is to reach from starting point to end point in minimum time possible, while avoiding slipping and keeping very low tracking error. We evaluate the performance of different path planners for this task. Tracking error te is taken as the log of mean squared error given by (20), where $x_{i,p}$, $y_{i,p}$, $x_{i,a}$, $y_{i,a}$ denote the planned and actual positions of the robot for x and y respectively, and n denotes the number of positions evaluated.

$$te = \log \frac{\sum_0^1 \sqrt{(x_{i,p} - x_{i,a})^2 + (y_{i,p} - y_{i,a})^2}}{n} \tag{27}$$

Fig. 6 compares the generated trajectory for various controllers for a fixed starting and ending point. Our approach takes into account the velocity and orientation of the robot at the end point. Excluding Quintic[10], in all other methods, the robot first reaches the end point at a high velocity,

TABLE I

COMPARISON OF OUR APPROACH WITH VARIOUS OTHER ALGORITHMS

Planner	Time(s)	te	Avg. Velocity(cm/s)
PController[3]	5.45	5.720	34.232
CMUnited[4]	**2.175**	7.137	**99.149**
S-curve[2]	2.675	6.634	83.338
Polar-Bidirectional[1]	4.19	4.836	42.536
Dynamic Window[6]	2.8	7.067	85.049
Quintic[10]	2.472	**4.6313**	90.470
Proposed approach	**2.2309**	**4.024**	**96.903**

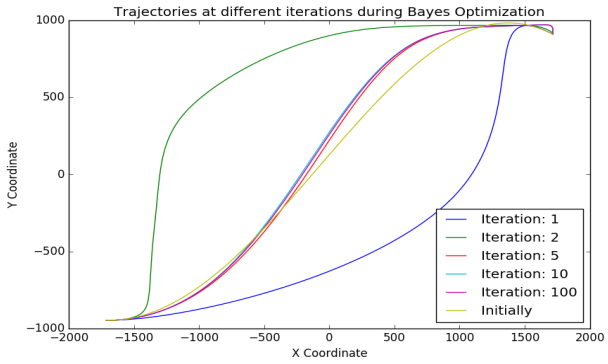

Fig. 7. Generated trajectories at different iterations during trajectory optimisation

over shoots and continues an oscillatory motion trying to reach the end point. Our approach is significantly better than other approaches as summarised by Table I. It has the least tracking error which is order of magnitudes better, while also minimising the time taken to reach the destination. Fig. 7 shows generated trajectories at different iterations during trajectory optimization, wherein the optimised trajectory has smoother turns leading to minimum traversal time. Also, Bayesian optimisation converges to minimum in very few iterations. Consequently, ball handling is improved during a match and no slipping is observed. The robot could now take very sharp and sudden turns. Due to low tracking errors, ball interception was also improved. This facilitated efficient high level behaviours such as defense, attack and ball interception.

APPENDIX

A. Curvature Derivatives

$$A(u) = y'''(u)x'(u) - x'''(u)y'(u) \tag{28}$$

$$B(u) = x'(u)x'(u) + y'(u)y'(u) \tag{29}$$

$$C(u) = x'(u)x''(u) + y'(u)y''(u) \tag{30}$$

$$\kappa'(u) = \frac{A}{B^{\frac{3}{2}}} - \frac{3\kappa(u)B(u)^{\frac{3}{2}}C(u)}{B^{\frac{5}{2}}} \tag{31}$$

ACKNOWLEDGMENT

We thank Prof. Sudeshna Sarkar, Prof. Alok Kanti Deb, and Prof. Dilip Kumar Pratihar for their constant guidance and support as co-Principal Investigators of KRSSG. We also thank all the alumni and present members of KRSSG especially Kumar Abhinav, Dhananjay Yadav, and Madhav Mantri for addressing game play, mechanical and embedded challenges in robot soccer.

REFERENCES

[1] A. De Luca, G. Oriolo, and M. Vendittelli, "Control of wheeled mobile robots: An experimental overview," in *Ramsete*. Springer, 2001, pp. 181–226.

[2] K. D. Nguyen, T.-C. Ng, and I.-M. Chen, "On algorithms for planning s-curve motion profiles," *International Journal of Advanced Robotic Systems*, vol. 5, no. 1, pp. 99–106, 2008.

[3] W. D. J. Dierssen, "Motion planning in a robot soccer system," *A Master's Thesis, Language, Knowledge and Interaction Group Department of Computer Science University of Twente The Netherlands*, 2003.

[4] M. Bowling and M. Veloso, "Motion control in dynamic multi-robot environments," in *Computational Intelligence in Robotics and Automation, 1999. CIRA'99. Proceedings. 1999 IEEE International Symposium on*. IEEE, 1999, pp. 168–173.

[5] O. Brock and O. Khatib, "High-speed navigation using the global dynamic window approach," in *Robotics and Automation, 1999. Proceedings. 1999 IEEE International Conference on*, vol. 1. IEEE, 1999, pp. 341–346.

[6] M. Seder and I. Petrovic, "Dynamic window based approach to mobile robot motion control in the presence of moving obstacles," in *Proceedings 2007 IEEE International Conference on Robotics and Automation*. IEEE, 2007, pp. 1986–1991.

[7] K. Jolly, R. S. Kumar, and R. Vijayakumar, "A bezier curve based path planning in a multi-agent robot soccer system without violating the acceleration limits," *Robotics and Autonomous Systems*, vol. 57, no. 1, pp. 23–33, 2009.

[8] A. Sahraei, M. T. Manzuri, M. R. Razvan, M. Tajfard, and S. Khoshbakht, "Real-time trajectory generation for mobile robots," in *Congress of the Italian Association for Artificial Intelligence*. Springer, 2007, pp. 459–470.

[9] Z. Shiller and Y.-R. Gwo, "Dynamic motion planning of autonomous vehicles," *IEEE Transactions on Robotics and Automation*, vol. 7, no. 2, pp. 241–249, 1991.

[10] B. Lau, C. Sprunk, and W. Burgard, "Kinodynamic motion planning for mobile robots using splines," in *2009 IEEE/RSJ International Conference on Intelligent Robots and Systems*. IEEE, 2009, pp. 2427–2433.

[11] R. Martinez-Cantin, "Bayesopt: a bayesian optimization library for nonlinear optimization, experimental design and bandits." *Journal of Machine Learning Research*, vol. 15, no. 1, pp. 3735–3739, 2014.

[12] J. A. Nelder and R. Mead, "A simplex method for function minimization," *The computer journal*, vol. 7, no. 4, pp. 308–313, 1965.

[13] S. Zickler, T. Laue, O. Birbach, M. Wongphati, and M. Veloso, "Ssl-vision: The shared vision system for the robocup small size league," in *Robot Soccer World Cup*. Springer, 2009, pp. 425–436.

[14] M. I. Ribeiro, "Kalman and extended kalman filters: Concept, derivation and properties," *Institute for Systems and Robotics*, vol. 43, 2004.

[15] A. Savitzky and M. J. Golay, "Smoothing and differentiation of data by simplified least squares procedures." *Analytical chemistry*, vol. 36, no. 8, pp. 1627–1639, 1964.

[16] A. Visioli, "Tuning of pid controllers with fuzzy logic," *IEE Proceedings-Control Theory and Applications*, vol. 148, no. 1, pp. 1–8, 2001.

[17] M. Lepetič, G. Klančar, I. Škrjanc, D. Matko, and B. Potočnik, "Time optimal path planning considering acceleration limits," *Robotics and Autonomous Systems*, vol. 45, no. 3, pp. 199–210, 2003.

[18] G. Farin, *Curves and surfaces for computer-aided geometric design: a practical guide*. Elsevier, 2014.

[19] S. Bochkanov and V. Bystritsky, "Alglib," 2013.

[20] R. Piessens, E. de Doncker-Kapenga, C. W. Überhuber, and D. K. Kahaner, *Quadpack: a subroutine package for automatic integration*. Springer Science & Business Media, 2012, vol. 1.

[21] B. Gough, *GNU scientific library reference manual*. Network Theory Ltd., 2009.
[22] H. Wang, J. Kearney, and K. Atkinson, "Arc-length parameterized spline curves for real-time simulation," in *5th international conference on Curves and Surfaces*, 2002.
[23] M. Walter and A. Fournier, "Approximate arc length parameterization," in *Proceedings of the 9th Brazilian symposium on computer graphics and image processing*. Citeseer, 1996, pp. 143–150.
[24] C. Sprunk, "Planning motion trajectories for mobile robots using splines," *University of Freiburg*, 2008.
[25] M. Minoux, *Mathematical programming: theory and algorithms*. John Wiley & Sons, 1986.
[26] J. Snoek, H. Larochelle, and R. P. Adams, "Practical bayesian optimization of machine learning algorithms," in *Advances in neural information processing systems*, 2012, pp. 2951–2959.
[27] C. E. Rasmussen, "Gaussian processes for machine learning," 2006.
[28] M. Stein, "Large sample properties of simulations using latin hypercube sampling," *Technometrics*, vol. 29, no. 2, pp. 143–151, 1987.
[29] G. Klančar and I. Škrjanc, "Tracking-error model-based predictive control for mobile robots in real time," *Robotics and Autonomous Systems*, vol. 55, no. 6, pp. 460–469, 2007.